Phase transitions and accidental degeneracy in nonlinear spin systems

Octavio Castaños, Ramón López-Peña, and Jorge G. Hirsch
Instituto de Ciencias Nucleares, Universidad Nacional Autónoma de México, Apartado Postal 70-543 México 04510 Distrito Federal

Enrique López-Moreno
Departamento de Física, Facultad de Ciencias, Universidad Nacional Autónoma de México, Apartado Postal 70-348 México 04511 Distrito Federal

(Received 27 April 2005; published 11 July 2005)

A characterization of phase transitions and related accidental degeneracies is presented for a general spin Hamiltonian containing linear and quadratic terms. The existence of first-, second-, and third-order phase transitions is exhibited. Regions in the control parameters space are found where crossings and anticrossings of quantum levels take place. The possibility of closely reproducing the ground and first excited states using even- and odd-spin coherent states is emphasized.

DOI: 10.1103/PhysRevB.72.012406 PACS number(s): 75.10.−b, 05.70.Fh, 21.60.Fw, 42.50.Dv

Arrays of interacting spins have attracted much attention in recent years. Entanglement of quantum states and phase transtions can be studied in these relatively simple systems. Trapped ions interacting with lasers may undergo a variety of phase transitions, representing an analog quantum simulator of spin systems.[1] Entanglement estimators represent a way of detecting quantum phase transitions in anisotropic $S=1/2$ antiferromagnetic chains.[2] A diverging entanglement length in the Ising spin model illustrates the quantum phase transition.[3] The behavior of critical entanglement in spin systems[4] is analogous to that of entropy in conformal field theories.[5] Networks of globally coupled oscillators exhibit phase transitions from incoherent to coherent states.[6] Quantum phase transitions in mesoscopic systems, defined for infinite number of particles N persist even for moderate N.[7]

In nuclear physics, it was determined since the beginning of the 1980s that the Bohr-Mottelson liquid drop model is the classical limit of the interacting boson model (IBM).[8] Equilibrium shapes associated to dynamical symmetries and its shape transitions were studied. The correspondence between classical and quantum variables was established constructing the energy surface as the expectation value of the IBM Hamiltonian with respect to the coherent states of the model.[9]

The classical theory of phase transitions within the catastrophe formalism[10,11] demonstrates that a shape phase transition occurs when the control parameters of the Hamiltonian are varied and the deformation variables jump from one critical branch to another.[12] Quantum phase transitions between spherical, prolate, oblate, and γ-unstable nuclear ground-state shapes have been found in the IBM,[13] with an analogy between the IBM results and predictions of the Landau theory of phase transitions in classical thermodynamics.[14–16]

In this paper, we study the geometric interpretation and the degeneracy of the nonlinear spin Hamiltonian

$$H = 2\omega J_0 + \frac{\lambda}{2}(J_+^2 + J_-^2) + \frac{\gamma}{2}(J_+J_- + J_-J_+), \tag{1}$$

where the operators J_0, $J_\pm$ denote the spherical components of angular momentum operators and λ and γ are real parameter strengths. This model Hamiltonian has been very successful in several fields of physics. In nuclear physics, this Hamiltonian is known as the Meshkov-Glick-Lipkin (MGL) model[17] and can represent a two-level system of identical particles interacting through particle-particle and particle-hole channels, where phase transitions from single particle to collective motion can be visualized.[18] It can also describe a system with proton and neutron quasiparticles in the presence of neutron-proton pairing.[19] In the field of quantum optics, this Hamiltonian allowed Kitagawa and Ueda[20] to produce spin squeezed states.

The classical limit of this system is established by studying the expectation value of the Hamiltonian in the $SU(2)$ coherent states. This expectation value defines the energy surface and it is analyzed using the catastrophe theory formalism. Once the critical points are found, it is necessary to determine which of them belong to bifurcations or Maxwell sets. The union of these sets defines the *separatrix* of the system, which classifies the regions in the essential parameters space where there are phase transitions and its order, according to the thermodynamic Ehrenfest classification.

The spin coherent states are defined by[21]

$$|\zeta\rangle = (1+|\zeta|^2)^{-J}\exp(\zeta^* J_+)|J,-J\rangle, \tag{2}$$

where $\zeta=\tan(\theta/2)\exp(i\phi)$ and J is associated with the number of particles. After making a shift and a magnification, the expectation value of the Hamiltonian between coherent states can be written as

$$\varepsilon(\theta,\phi) = \frac{\langle\zeta|H|\zeta\rangle - \gamma J}{\omega J},$$

$$= -2\cos\theta + \gamma_x \sin^2\theta\cos^2\phi + \gamma_y \sin^2\theta\sin^2\phi, \tag{3}$$

where the parameters γ_x and γ_y are defined by

$$\gamma_x = \frac{2J-1}{2\omega}(\gamma+\lambda), \quad \gamma_y = \frac{2J-1}{2\omega}(\gamma-\lambda). \tag{4}$$

Trial states with good parity properties can be built as even and odd spin coherent states given by

$$|\zeta\rangle_{\pm} = \frac{1}{\sqrt{2(1 \pm (\cos\theta)^{2J}}}(|\zeta\rangle \pm |-\zeta\rangle). \tag{5}$$

The expectation value of the Hamiltonian between the even (+) and odd (−) spin coherent states takes the form

$$\varepsilon_{\pm}(\theta,\phi) = \frac{{}_{\pm}\langle\zeta|H|\zeta\rangle_{\pm} - \gamma J}{\omega J},$$

$$= \varepsilon(\theta,\phi)F_{\pm}(\theta,J) \mp (\gamma_x + \gamma_y)G_{\pm}(\theta,J), \tag{6}$$

where the functions F, G are given by the expressions

$$F_{\pm}(\theta,J) = \frac{1 \pm (\cos\theta)^{2J-2}}{1 \pm (\cos\theta)^{2J}},$$

$$G_{\pm}(\theta,J) = \frac{(\sin\theta)^2(\cos\theta)^{2J-2}}{1 \pm (\cos\theta)^{2J}}. \tag{7}$$

The same shift and magnification are chosen for the three energy surfaces to allow a simple comparison between them. When $J \to \infty$, the functions $F_{\pm}$ go to the unity, and functions $G_{\pm}$ go to zero. From now on, the functions ε, ε_+, and ε_- denote normal, even, and odd energy surfaces and in this asymptotic limit they are equivalent.

An analysis of the normal energy surface (3), when the control parameters γ_x and γ_y are varied, allows the determination of critical points, its degeneracy, the bifurcation sets, and the loci in the control parameters space where phase transitions occur from one local critical point to another. One can organize all the critical points according to their stability within the control parameters space.

The critical points of the energy surface are found by solving the equation $\nabla\varepsilon(\theta,\phi)=0$. From this expression, it is immediate that the poles (*i*) $\theta_c=0$ and (*ii*) $\theta_c=\pi$ are critical points for any values of the parameters γ_x and γ_y. For this reason they are called *fundamental roots*. A Taylor series expansion around these *fundamental roots* determines that the system has a fourth-order germ,[11] implying that there exits at most triple degeneracy in the critical points.[22] Besides, there are additional critical points which are

$$(iii)\ \left[\theta_c = \arccos\left(\frac{-1}{\gamma_x}\right),\quad \phi_c = 0\right],\quad \text{if } |\gamma_x| > 1,$$

$$(iv)\ \left[\theta_c = \arccos\left(\frac{-1}{\gamma_x}\right),\quad \phi_c = \pi\right],\quad \text{if } |\gamma_x| > 1,$$

$$(v)\ \left[\theta_c = \arccos\left(\frac{-1}{\gamma_y}\right),\quad \phi_c = \frac{\pi}{2}\right],\quad \text{if } |\gamma_y| > 1,$$

$$(vi)\ \left[\theta_c = \arccos\left(\frac{-1}{\gamma_y}\right),\quad \phi_c = \frac{3\pi}{2}\right],\quad \text{if } |\gamma_y| > 1,$$

$$(vii)\ \left[\theta_c = \arccos\left(\frac{-1}{\bar{\gamma}}\right),\quad \phi_c = \phi\right],\quad \text{if } |\bar{\gamma}| > 1,$$

where $\bar{\gamma}$ denotes the common value $\gamma_y=\gamma_x$. The functional form of the normal energy surface at the critical points is

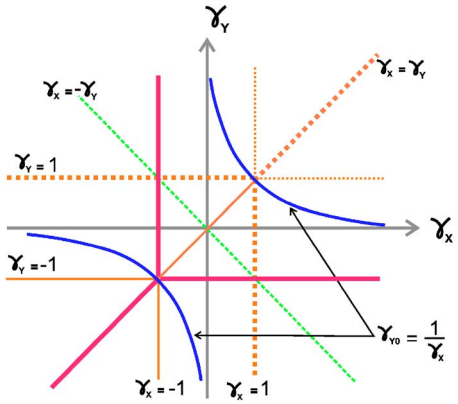

FIG. 1. (Color online) The bifurcation sets are plotted together with the straight lines $\gamma_y=-\gamma_x$, $\gamma_y=\gamma_x$, with $|\gamma_x| \leq 1$, and the hyperbola $\gamma_{y0}=1/\gamma_x$. The bifurcation sets associated to phase transitions between minima are shown with thick lines while those related with maxima are displayed by thick dotted lines. A reflection along the straight lines $\gamma_y=\pm\gamma_x$ yields related energy spectra.

$$\varepsilon(0,0) = -2, \quad \varepsilon(\pi,0) = 2, \quad \varepsilon(\theta_c,\phi_c) = \Gamma + \frac{1}{\Gamma}, \tag{8}$$

where we define

$$\Gamma = \begin{cases} \gamma_x, & \text{when } \phi_c = 0 \text{ or } \pi, \\ \gamma_y, & \text{when } \phi_c = \dfrac{\pi}{2} \text{ or } \dfrac{3\pi}{2}, \\ \bar{\gamma}, & \text{when } \gamma_x = \gamma_y = \bar{\gamma}. \end{cases} \tag{9}$$

To have the minimal classical energy surface, the following additional conditions on the control parameters space must be satisfied:

$$\text{for } \Gamma = \gamma_x, \quad \gamma_x < -1, \quad \text{and } \gamma_x < \gamma_y,$$

$$\text{for } \Gamma = \gamma_y, \quad \gamma_y < -1, \quad \text{and} \quad \gamma_y < \gamma_x,$$

$$\text{for } \Gamma = \bar{\gamma}, \quad \bar{\gamma} < -1.$$

The Maxwell sets[11] are the loci in parameters space for which the classical energies at two or more critical points are equal, and under small changes of the control parameters satisfy the Clausius-Clapeyron equations

$$\{\partial\varepsilon^{(1)}/\partial\gamma_\alpha - \partial\varepsilon^{(2)}/\partial\gamma_\alpha\}\delta\gamma_\alpha = 0. \tag{10}$$

The subindex α takes the values x and y; $\varepsilon^{(1)}$ and $\varepsilon^{(2)}$ denote the two degenerate energies at critical points. When a Maxwell set is crossed, the energy surface jumps from one critical branch to another, and phase transitions take place for $|\Gamma| \geq 1$. Phase transitions for the minimum values of the classical energy surface can only happen for $\Gamma \leq -1$. In Fig. 1 they correspond to the regions where $\gamma_x \leq -1$ and $\gamma_y \leq -1$.

Bifurcation sets are the loci in parameters space where the function ε changes because equilibria points are either created or destroyed. They are obtained from the vanishing of the determinant of the matrix of second derivatives of ε evaluated at the critical points, that is, $\det \varepsilon_{ij}=0$, with $i,j = \theta,\phi$. The parameter values that satisfy these conditions are

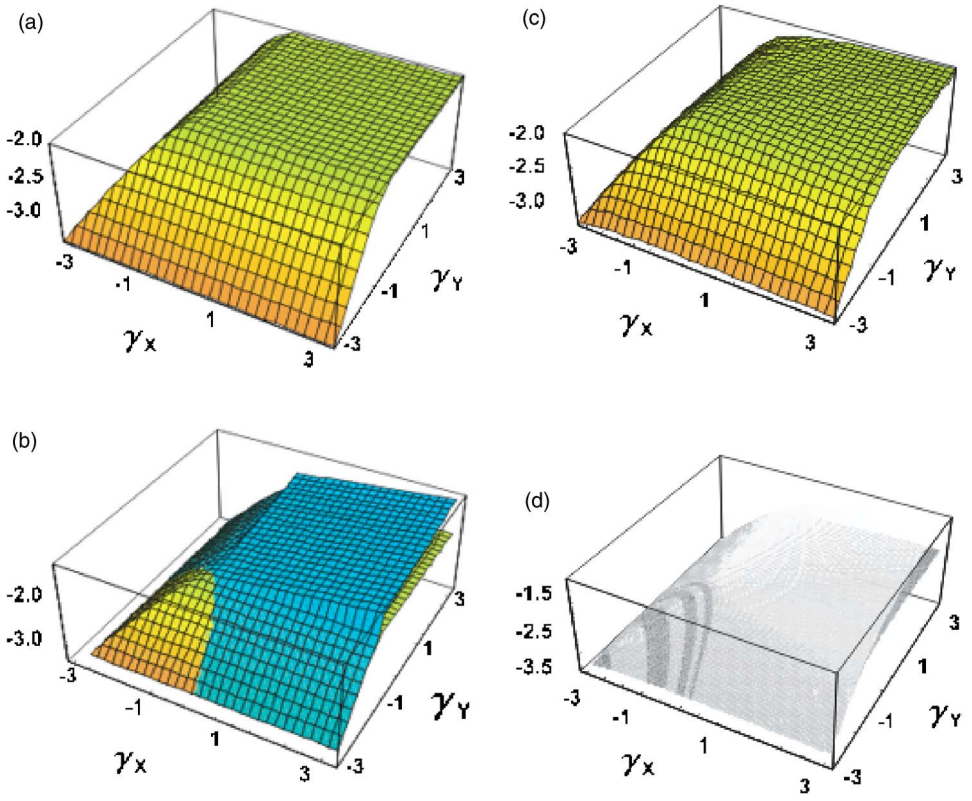

FIG. 2. (Color online) In (a), the even energy surface is plotted for $N=20$ and the ranges of the control parameters $-3\leqslant\gamma_x\leqslant 3$ and $-3\leqslant\gamma_y\leqslant 3$. In (b), the superposition of the minima even and odd energy surfaces is displayed for the same range of parameters. In (c), the minimum energy of the Hamiltonian is plotted for the exact even eigenstates, while in (d), the superposition of minima for the exact even and odd eigenstates is shown.

$$\gamma_x=\pm 1;\quad \gamma_y=\pm 1;\quad \gamma_x=\gamma_y \text{ with } |\gamma_x|\geqslant 1. \tag{11}$$

They are shown in Fig. 1. A second-order phase transition of the Ginzburg-Landau type takes place when the straight lines $\gamma_x=-1$, $\gamma_y=-1$ and the point $(\gamma_x,\gamma_y)=(-1,-1)$ are crossed. The crossing of the straight line $\gamma_y=\gamma_x$ yields a first-order transition. Special attention must be given to the crossing of the cusp point $(\gamma_x,\gamma_y)=(-1,-1)$ along the straight line $\gamma_y=-\gamma_x-2$ because in that case there is a third-order phase transition, related to a convergence of second-order phase transitions.

In Fig. 2(a), the minimum values of the even energy surface are displayed. Notice that $\varepsilon_+\approx -2$ for $\gamma_x\geqslant -1$ and $\gamma_y\geqslant -1$; one can also see visible changes along the straight lines $\gamma_x=-1$, $\gamma_y=-1$, and $\gamma_y=\gamma_x$ closely related with the phase transitions discussed for the normal energy surface. In Fig. 2(b), the minimum values of the even and odd energy surfaces are plotted together. For $\gamma_x\geqslant -1$ and $\gamma_y\geqslant -1$ only the odd energy surface ε_- is observed as a flat surface with $\varepsilon_-\approx -1$ with a small slope. At the bifurcation sets, for $\gamma_x<-1$ and $\gamma_y<-1$ the slope changes suddenly and the odd energy surface starts decreasing faster than the even one. At the hyperbola $\gamma_{yk}=1/\gamma_x$, there is a crossing between ε_+ and ε_-. Beyond this curve the minimum odd energy surfaces has a lower energy than the minimum even energy surface, shown with light gray in Fig. 2(b).

A deeper understanding of the behavior of the system is obtained by analyzing the quantum solution of the Hamiltonian (1). After the same shift and scaling, it can be rewritten as

$$H=\frac{J(\gamma_x+\gamma_y)}{2J-1}+\frac{2}{J}J_0-\frac{(\gamma_x+\gamma_y)}{J(2J-1)}J_0^2+\frac{\gamma_x-\gamma_y}{2J(2J-1)}(J_+^2+J_-^2). \tag{12}$$

Notice that under reflections along the straight lines $\gamma_y=\gamma_x$ and $\gamma_y=-\gamma_x$ the Hamiltonian yields the same energy spectrum and an inverted energy spectrum, respectively. Therefore in the $\gamma_x-\gamma_y$ plane, it is sufficient to study the quantum solutions only one quadrant of the control parameters space (cf. Fig. 1).

When the case with maximum symmetry is considered, the number of particles is twice the value of the angular momentum $N=2J$. Exact eigenvalues and eigenvectors are obtained in the angular momentum basis states

$$|Nn\rangle=\sqrt{\frac{(N-n)!}{(N)!(n)!}}J_+^n|N0\rangle, \tag{13}$$

where $n=J+M$, and with n varying from 0 to N. The state $|N0\rangle$ is the unperturbed ground state, i.e., the ground state when $\gamma_x=\gamma_y=0$. In this case all the particles occupy the lowest level. Since the Hamiltonian (12) has nonvanishing matrix elements only between states (13) with $n\rightarrow n,n\pm 2$, its eigenfunctions can be written in terms of linear combinations of states with even or odd values of n. The even and odd exact lowest energy states correspond to the ground or the first excited states of the system.

For the case $\gamma_x=\gamma_y=\bar{\gamma}$, the energy spectrum is given by

$$E_n(N)=\frac{N\bar{\gamma}}{N-1}+\frac{4}{N}\left(n-\frac{N}{2}\right)-\frac{2\bar{\gamma}}{N-1}\left(n-\frac{N}{2}\right)^2. \tag{14}$$

There are crossings (degeneracies) between the quantum solutions with different or the same parity when

$$E_k(N) = E_{k+1}(N) \text{ or } E_l(N) = E_{l+2}(N). \quad (15)$$

In the first case, the condition

$$\bar{\gamma}_k^{(1)} = -\frac{N-1}{N-2k-1} \quad (16)$$

is obtained, with $k=0,1,\ldots,N-1$, while in the second, one gets

$$\bar{\gamma}_l^{(2)} = -\frac{N-1}{N-2l-2}, \quad (17)$$

with $l=0,1,\ldots,N-2$. These are all the $\bar{\gamma}$ values where there is degeneracy for the diagonal case. Thus for a given number of particles N, there are $2N-2$ energy crossings.

There are J or $J+1/2$ crossings between the ground and first excited states, according to the integer or half integer value of the angular momentum, respectively. These crossings occur only for negative values of $\bar{\gamma}$, in agreement with the condition of the minima of the classical energies.

For $\gamma_y \neq \gamma_x$, the crossings and anticrossings of the quantum levels are described by the hyperbolae

$$\gamma_{yk} = \frac{(\bar{\gamma}_k^{(1)})^2}{\gamma_x}, \quad \gamma_{yl} = \frac{(\bar{\gamma}_l^{(2)})^2}{\gamma_x}, \quad (18)$$

where $\bar{\gamma}_k^{(1)}$ and $\bar{\gamma}_l^{(2)}$ are given in Eqs. (16) and (17) respectively. The first expression is associated to the crossings of the energy levels of different parity, while the second one determines anticrossings of quantum levels of the same parity. If $\gamma_{yk}=\gamma_x$ or $\gamma_{yl}=\gamma_x$ in the last expressions, the crossings for the diagonal cases (16) and (17) are recovered. It is straightforward that there is not degeneracy for $\gamma_{yk}=-\gamma_x$.

In Fig. 2(c) the lowest energies for even eigenstates are shown while in Fig. 2(d) the lowest energies for both even and odd eigenstates are displayed together. The number of darker bands depends on the number of particles and show regions where the ground state has odd parity. Each crossing hyperbolae is given by γ_{yk}. The similarity with the corresponding plot for the classical energy is evident. That is, the bifurcation sets $\gamma_x=-1$, $\gamma_y=-1$, and the cusp[11] $(\gamma_x,\gamma_y)=(-1,-1)$ can be seen in all the figures. In the lower part, the phase transitions and degeneracies are shown. For the classical energies, one hyperbola shows the crossings of even and odd energy surfaces. This hyperbola always coincides with the first degeneracy region of the exact quantum result. When the number of particles goes to ∞, only the phase transitions associated to the *separatrix* of the normal energy surface remain.

The *separatrix* is fundamental to determine the stability properties, phase transitions, and even the accidental degeneracy of the nonlinear spin Hamiltonian. The bifurcation sets displayed by the thick continuous line in Fig. 1 separate the single particle motion from the collective one. For $\gamma_x<-1$ and $\gamma_y<-1$ the eigenstates are constituted by many components of the angular momentum basis states, while for the region $\gamma_x \geqslant -1$ and $\gamma_y \geqslant -1$, only one component is dominant. In the interior region of the hyperbolae there is not degeneracy whereas in the exterior part, degeneracy is present. For negative values of γ_x and γ_y, there are crossings between quantum levels with negative energy, meanwhile for positive values, crossings occur between energy levels with positive energy. The hyperbolae γ_{yk}, Eq. (18) indicate the set of points in the γ_x-γ_y plane where there are degeneracies, i.e., crossings between exact even and odd energy levels. The label k of these functions is related with the number of degenerate pairs of energy levels. That is, for $k=0$ there is one degenerate pair; for $k=1$, there are two degenerate pairs; and so on. The hyperbolae γ_{yl} Eq. (18) determine the region where there are anticrossings between pairs of exact even or odd energy levels. There are degeneracy only by the existence of a symmetry, that is, at the points $\gamma_{yl}=\bar{\gamma}_l^{(2)}$. The evolution of the energy surfaces as a function of the control parameters and its relation with the exact quantum states will be discussed in a future work.

This work was partially supported by CONACyT.

[1] D. Porras and J. I. Cirac, Phys. Rev. Lett. **92**, 207901 (2004).
[2] T. Roscilde, P. Verrucchi, A. Fubini, S. Haas, and V. Tognetti, Phys. Rev. Lett. **93**, 167203 (2004).
[3] F. Verstraete, M. Popp, and J. I. Cirac, Phys. Rev. Lett. **92**, 027901 (2004).
[4] S. Dusuel and J. Vidal, Phys. Rev. Lett. **93**, 237204 (2004).
[5] G. Vidal, J. I. Latorre, E. Rico, and A. Kitaev, Phys. Rev. Lett. **90**, 227902 (2003).
[6] C. von Cube, S. Slama, D. Kruse, C. Zimmermann, P. W. Courteille, G. R. M. Robb, N. Piovelli, and R. Bonifacio, Phys. Rev. Lett. **93**, 083601 (2004).
[7] F. Iachello and N. V. Zamfir, Phys. Rev. Lett. **92**, 212501 (2004).
[8] J. N. Ginocchio and M. W. Kirson, Phys. Rev. Lett. **44**, 1744 (1980); A. E. L. Dieperink, O. Scholten, and F. Iachello, *ibid.* **44**, 1747 (1980).
[9] R. Gilmore, J. Math. Phys. **20**, 891 (1979); R. Gilmore, C. M. Bowden, and L. M. Narducci, Phys. Rev. A **12**, 1019 (1975).
[10] D. H. Feng, R. Gilmore, and S. R. Deans, Phys. Rev. C **23**, 1254 (1981).
[11] R. Gilmore, *Catastrophe Theory for Scientists and Engineers* (Wiley, New York, 1981).
[12] E. López-Moreno, and O. Castaños, Rev. Mex. Fis. **42**, 163 (1996); Phys. Rev. C **54**, 2374 (1996).
[13] E. López-Moreno and O. Castaños, Rev. Mex. Fis. **44**, S48 (1998); J. E. García-Ramos, J. M. Arias, J. Barea, and A. Frank, Phys. Rev. C **68**, 024307 (2003).
[14] J. Jolie, P. Cejnar, R. F. Casten, S. Heinze, A. Linnemann, and V. Werner, Phys. Rev. Lett. **89**, 182502 (2002).
[15] F. Iachello, Phys. Rev. Lett. **85**, 3580 (2000); **87**, 052502 (2001).
[16] P. Cejnar, S. Heinze, and J. Jolie, Phys. Rev. C **68**, 034326 (2003).
[17] H. J. Lipkin, N. Meshkov, and A. J. Glick, Nucl. Phys. **62**, 188 (1965).
[18] P. Ring and P. Schuck, *The Nuclear Many-Body Problem* (Springer-Verlag, New York, 1980).
[19] J. G. Hirsch, O. Civitarese, and M. Reboiro, Phys. Rev. C **60**, 024309 (1999).
[20] M. Kitagawa and M. Ueda, Phys. Rev. A **47**, 5138 (1993).
[21] F. T. Arecchi, E. Courtens, R. Gilmore, and H. Thomas, Phys. Rev. A **6**, 2211 (1972).
[22] O. Castaños, E. López-Moreno, R. López-Peña, Rev. Mex. Fis. **49** S4, 15 (2003).